Composite Nanocrystals

DOI: 10.1002/anie.201102994

Triple-Layer (Au@Perylene)@Polyaniline Nanocomposite: Unconventional Growth of Faceted Organic Nanocrystals on Polycrystalline Au**

*Melinda Sindoro, Yuhua Feng, Shuangxi Xing, Hai Li, Jun Xu, Hailong Hu, Cuicui Liu, Yawen Wang, Hua Zhang, Zexiang Shen, and Hongyu Chen**

Nanocrystals are of critical significance for nanoscience and nanotechnology.[1] Unlike the fabrication of macroscopic objects, constructing flat surfaces on the nanoscale almost entirely relies on the growth of crystal facets, that is, the intrinsic self-assembly of atoms or molecules. Thus, great efforts have been devoted to understanding the fundamentals of crystal growth and improving its structural complexity. So far, excellent control of nanocrystal facets and overall morphology has been demonstrated in many single-component systems,[1a] but facet control in multicomponent nanostructures remains a great challenge.[2]

Indeed, nanocrystals with incorporated foreign material have rarely been reported. In most cases, crystal growth occurred on one side of the seeds to give Janus (two-sided) nanoparticles,[3] as the two materials often do not have matching lattices and suitable interfacial energy.[1b,4] Only when the overcoating material was chosen to match the seed material could epitaxial growth establish lattice order throughout the resulting core/shell nanocrystals.[2a–d,4a] Limited by the requirements of epitaxial growth, most hybrid nanocrystals reported in the literature involved two inorganic materials (e.g., metal on metal[2–4]), while overgrowth of organic nanocrystals on inorganic seeds has so far not been demonstrated. Given the large differences between organic and inorganic materials, it is not easy to achieve lattice matching. Despite the challenges, expanding the scope of hybrid nanocrystals is of fundamental importance, as it allows the creation of complex nanostructures with crystal facets.

Here we report an unconventional crystal growth in which a dominant single-crystalline phase of perylene was grown on polycrystalline Au nanoparticles (AuNPs; Figure 1). This unusual growth process allows full encapsulation of precisely one Au seed in each organic nanocrystals. On the basis of intermediates isolated by encapsulation in polyaniline (PANI), we postulate that growth of perylene probably starts at one or a few nucleation sites on each AuNP before completely engulfing it. The growth of perylene on the AuNP tolerates defects due to molecular distortion or reorientation,

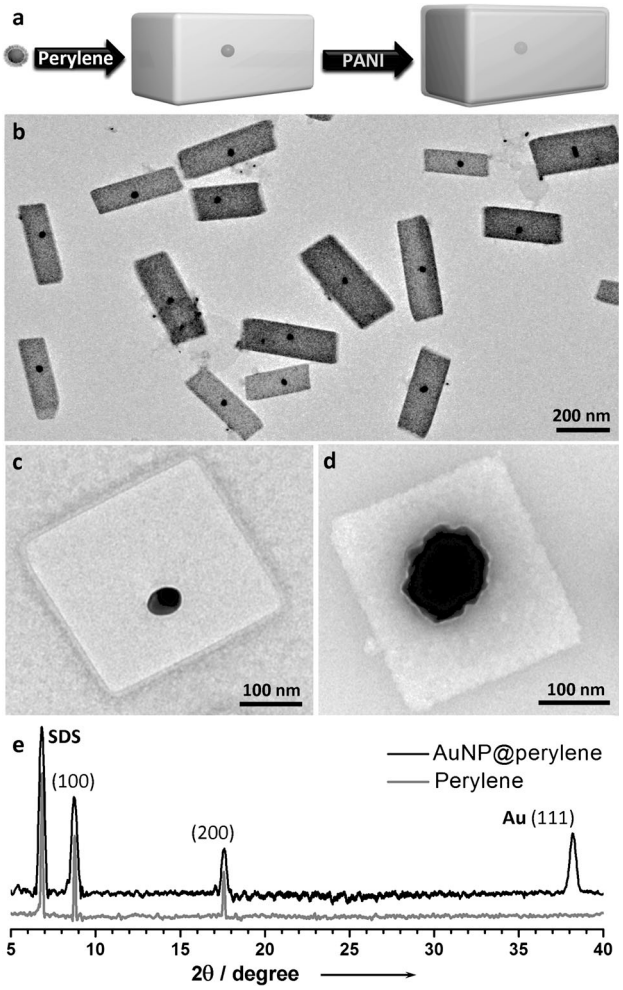

Figure 1. Triple-layer (Au@perylene)@PANI nanocomposites. a) Schematics of the two-step synthesis. b, c) TEM images of nanocomposites grown from 60 nm AuNPs. d) Nanocomposites grown from 100 nm AuNFs. e) XRD patterns of perylene and AuNP@perylene nanocrystals after background subtraction.

[*] M. Sindoro, Y. Feng, S. Xing, J. Xu, C. Liu, Y. Wang, Prof. H. Chen
Division of Chemistry and Biological Chemistry, Nanyang Technological University, 21 Nanyang Link, Singapore 637371 (Singapore)
E-mail: hongyuchen@ntu.edu.sg
Homepage: http://www.ntu.edu.sg/home/hongyuchen/
Dr. H. Li, Prof. H. Zhang
Division of Materials Science and Engineering, Nanyang Technological University, Singapore 639798 (Singapore)
H. Hu, Prof. Z. Shen
Division of Physics and Applied Physics, Nanyang Technological University, Singapore 637371 (Singapore)
S. Xing
Faculty of Chemistry, Northeast Normal University (P. R. China)

[**] The authors thank Ministry of Education, Singapore (ARC 13/09) for financial support.

Supporting information for this article is available on the WWW under http://dx.doi.org/10.1002/anie.201102994.

which is distinctly different from the growth of inorganic nanocrystals. This unusual tolerance was the key to obtaining the composite nanocrystals.

The AuNPs were first functionalized with perylene molecules to render them amenable for subsequent perylene deposition. Citrate-stabilized AuNPs[5] were incubated with an excess of perylene in DMF at 60 °C for 2 h. The solution was centrifuged to remove the supernatant, and the isolated NPs were transferred to an aqueous solution of sodium dodecyl sulfate (SDS). The color of the solution remained red, indicating the absence of significant aggregation.[6] To confirm ligand exchange on the AuNPs, the resulting colloid was characterized by Raman scattering, which showed characteristic surface-enhanced Raman scattering (SERS) peaks of perylene at 1559, 1362, and 1285 cm^{-1}.[7] In comparison, perylene by itself at equivalent concentration did not give noticeable Raman peaks. Direct TEM characterization of the SDS/perylene-stabilized AuNPs showed large aggregates, but it was not clear whether aggregation was due to the drying process of TEM sample preparation. Hence, we coated these colloidal NPs with PANI shells using our previously established method.[6b] After purification, the NPs were dried and characterized by TEM. Most of the observed AuNPs were singly encapsulated by polymer,[5] that is, the SERS signal of the original SDS/perylene-stabilized AuNPs was not caused by the hotspots[8] of a few aggregates.

Hence, incubation with perylene replaced the surface ligands on the AuNPs,[9] while SDS stabilized the perylene-functionalized AuNPs against aggregation in water. The resulting NPs were used as seeds, and a large excess of perylene in DMF was added to the aqueous solution, so that the insoluble perylene formed nanocrystals. The resulting products also cannot be directly characterized by TEM, as they tend to aggregate and undergo further crystal growth on drying. Thus, they were encapsulated in PANI shells[6b] and then isolated from the excess reactants and polymer. The product was still a messy mixture of (Au@perylene)@PANI, Au@PANI (80% of the AuNPs), and a small amount of perylene@PANI (7% of the perylene crystals).[5] To further clean up the sample, the Au@PANI was etched by KCN,[6b,10] and only the heavier (Au@perylene)@PANI was isolated by centrifugation. Figure 1b and c show the resulting sample of rhombohedral perylene crystals with a single AuNP at their center.

The PANI shell was confirmed on the basis of similar oxidation of aniline[2b,6b] and its SERS signals (Figure 2f). Under TEM, with a negative stain, the PANI shells of about 10 nm in thickness showed enough contrast to the perylene crystals to be observed (e.g., Figure 1c).

The PANI shells are known to be permeable[6b] and allow Au@PANI to be etched in less than 1 h. In contrast, the AuNPs embedded in (Au@perylene)@PANI were not etched for at least 3 d. The fact that these AuNPs are well protected suggests that they are completely embedded in the hydrophobic perylene nanocrystals, as opposed to half-encapsulation at their surface. Indeed, the AuNPs always appear at the center of perylene crystals despite the random crystal orientation. The proposal was further corroborated by additional AFM characterization.[5]

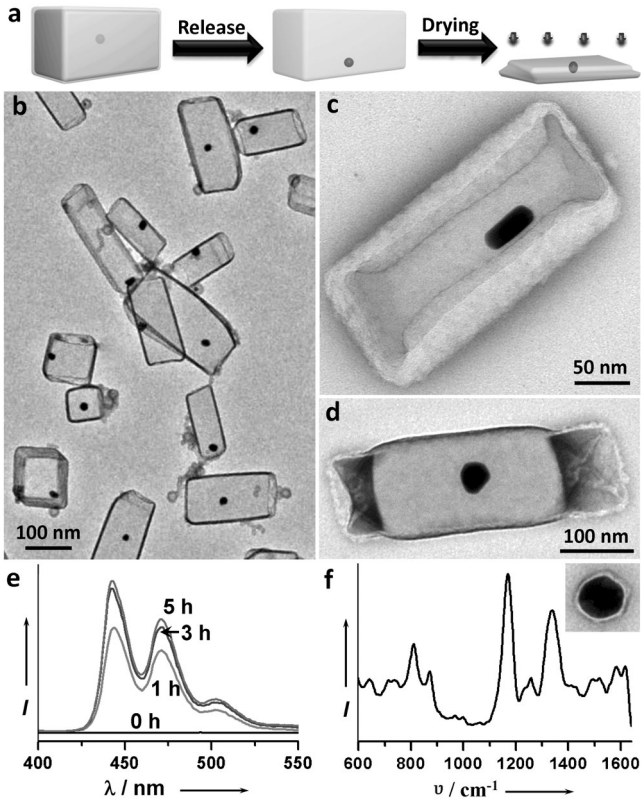

Figure 2. Controlled perylene release. a) Schematic illustration. b, c) TEM images of yoke/shell Au@PANI after complete release of perylene. d) TEM image of (Au@perylene)@PANI after partial release. e) Perylene fluorescence spectra ($\lambda_{ex} = 335$ nm). f) SERS of Au@PANI indicates PANI formation.

In the absence of AuNPs, perylene could form nanocrystals by itself.[11] However, the obtained crystals were more polydisperse in size, which could be attributed to continuous nucleation during the growth stage. In contrast, concurrent perylene growth on AuNP seeds led to more uniform crystal sizes.[12] Multiple AuNPs could also be incorporated in each perylene crystal[5] if they were induced to aggregate[6a] before perylene growth.

The polymer-enclosed Au@perylene heterocrystals must have been formed in the solution phase prior to polymerization. While most of the organic nanocrystals in Figure 1b showed ordered flat facets, they are clearly not single-crystalline: they contain at least one large defect, that is, the AuNP at their center. Additional small perylene domains may be embedded along with the AuNP, but they are indistinguishable under TEM. Nevertheless, the parallel facets and consistent crystal angles of the rhombohedral perylene crystals (>99%) are a clear indication for internal lattice order. Hence, we concluded that most of the Au@perylene crystals must contain a dominant single-crystalline perylene domain.

To confirm the composition of the organic crystals, powder XRD data (Figure 1e)[5] were collected from the isolated perylene and AuNP@perylene nanocrystals (without PANI shells). Both samples showed two peaks that can be assigned to α-perylene (100) and (200). In addition, a weak Au (111) peak was observed in the Au@perylene sample.

The perylene in (Au@perylene)@PANI can be viewed as a model hydrophobic drug[13] and it can be released on incubation with SDS micelles in water (Figure 2). Perylene fluorescence is quenched in the crystalline state.[14] During the course of release, characteristic perylene emission peaks[15] emerged (Figure 2e), which can be attributed to transfer of perylene molecules to the SDS micelles.[13a] After release, the PANI shells partially retained their regular shapes with the AuNPs still trapped inside (Figure 2b, c). The overall structure appeared more transparent under TEM, and the shell often collapsed inward to form a thick edge. The extent of perylene unloading could be tuned by adjusting the amount of SDS used. Partially dissolved perylene crystals were obtained, for which clear contrast can be observed between the residual crystal and the hollow collapsed polymer shell (Figure 2d). The correlation between the disappearance of nanocrystals and the emergence of perylene fluorescence signal was further confirmation of the identity of the crystals.

The AuNPs prepared by citrate reduction are known to be polycrystalline in nature. Thus, it is intriguing that a dominant single crystal can encapsulate a polycrystalline seed. To probe the limit of defect tolerance, we synthesized Au nanoflowers (AuNFs)[5] to ensure polycrystallinity. Among the obtained (AuNF@perylene)@PANI, the largest AuNF embedded in single-crystalline perylene (ca. 280 nm) was found to be 100 nm in diameter (Figure 1d), a vivid demonstration of how many defects an organic crystal can accommodate on the nanoscale.

To investigate possible hetero-epitaxy between perylene and Au, we used single-crystalline Au nanorods (AuNRs) as seeds. Similar AuNR@perylene were obtained, but some of the embedded AuNRs aggregated[5] when we tried to minimize the amount of residual cetyltrimethylammonium bromide. We used PANI encapsulation and KCN etching to clean up the sample, and surveyed only the singly encapsulated AuNRs (Figure 3). Among them, 21% were found in random orientation, 68% were aligned with their long axis perpendicular to the long axis of perylene crystal, and 11% were aligned in parallel.[5] Thus, there was clearly a preference for crystal alignment, which suggests hetero-epitaxy between perylene and Au.[19] This hetero-epitaxy was probably established in the initial stage when perylene first grew on Au. Since perylene growth could tolerate large defects, the later stage was likely insignificant. Hence, it is not surprising that the growth was able to accommodate the different facets of AuNRs and, in some cases, completely misaligned AuNRs.

Perylene growth was distinctly different from those reported in the literature. Typically, a crystal initiated from a spot on the seed (of a different material) and grew outward (Figure 4a).[2f,16] Unless the crystal and the seed have matching lattices,[2a–d,4a,17] the crystal will encounter numerous defects while wrapping around the seed and maintaining its overall lattice order. Such defects will greatly increase the interfacial energy and thus cause the crystal to reduce its contact with the seed. On the other hand, completely encapsulated core/shell nanostructures are common, particularly if the shell is made of polymer[6b] or amorphous material such as silica.[18] In these systems, simultaneous build up on the seed from all directions (Figure 4c) is possible because there is no need to maintain the lattice order within the shell material. As the seeds typically have more than one type of facets and edges that can serve as nucleation centers, even if the shell is capable of forming crystals, it will form polycrystalline structures. However, in our system, for the dominant single-crystalline perylene to grow around the seed, it must be able to tolerate a large number of defects along the Au/perylene interface (Figure 4b). It was thus surprising that these defects did not greatly increase the Au/perylene interfacial tension.

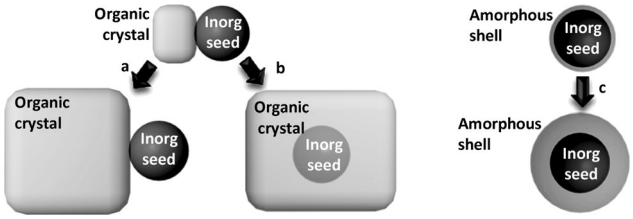

Figure 4. Schematic representations of the different modes in growing organic crystals or amorphous materials on inorganic seeds.

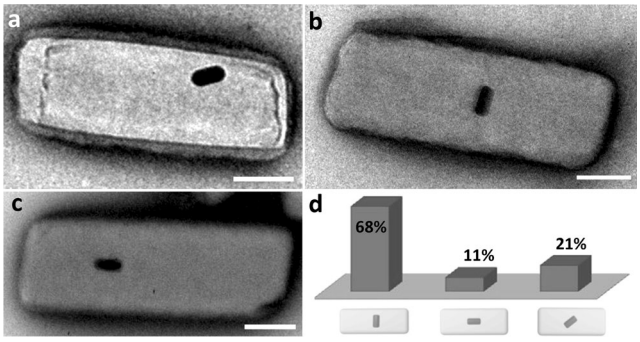

Figure 3. Crystal alignment. Typical TEM images showing alignment of the embedded AuNRs in triple-layer (AuNR@-perylene)@PANI. a) Random alignment. b, c) With long axis aligned perpendicular and parallel to the long axis of perylene crystal, respectively. d) Histogram showing alignment of the singly encapsulated AuNRs. Scale bars: 100 nm.

The stability of Au@perylene heterocrystals depends on the relative strength of the free energies at Au/perylene, Au/solvent, and perylene/solvent interfaces.[4c,d] If the interfacial energies are not suitable, partial encapsulation of the AuNP by perylene will most likely occur. Hence, the "wetting" property of perylene on the Au surface is of critical significance. While the perylene ligands adsorbed on the polycrystalline Au surface must have many different orientations that are not aligned with the perylene single crystal, they help to reduce the Au/perylene interfacial energy and to promote wetting. Control experiments showed that citrate-stabilized AuNPs were not incorporated in perylene crystals if they were directly used as seeds without being pre-incubated with perylene.

Indeed, even with prolonged incubation of AuNPs with perylene, not all AuNPs were incorporated in perylene crystals. Almost 80% of the AuNPs were found as

Au@PANI free of attached crystals. Control experiments were carried out before PANI encapsulation to separate the free AuNPs, which were then used as seeds in an additional cycle of perylene growth. Out of these AuNPs, 19% were found to be encapsulated in perylene crystals, which suggests that nucleation on the AuNPs was probably not selective but random. It is thus unlikely that those free AuNPs in the initial growth step were intrinsically unable to support perylene growth.

There is an alternative explanation for formation of single-crystalline perylene on Au: multiple small perylene crystals could initially form on all AuNPs, but some of them dissolved and were redeposited on the larger crystals (Ostwald ripening). This could nicely explain the absence of perylene crystals on some AuNPs. To test this hypothesis, AuNP@perylene with large perylene crystals (300 nm) and AuNF@perylene with partially formed small crystals (90 nm) were prepared separately. Then, the two samples were mixed and incubated for 12 h, before the products were trapped by PANI encapsulation and characterized by TEM. A large number of AuNFs were found with small perylene crystals still attached to them,[5] that is, equilibrium was not attained. Considering the very short crystal-growth time (< 30 min) for Au@perylene, Ostwald ripening cannot be the dominant factor in perylene crystal formation. Hence, the absence of perylene crystals on some AuNPs was likely the result of random nucleation.

By using PANI encapsulation as a means to trap growth intermediates, we explored the initial stages of perylene crystal formation by stepwise addition of small aliquots of perylene stock solution. Free AuNPs isolated in the form of Au@PANI were found in the samples of all stages,[5] in addition to the structures discussed below. Initially, one or two small perylene crystals were found attached to some AuNPs (Figure 5b; note: the degrees of growth were somewhat different among the individual NPs; see large-area views in the Supporting Information). On further perylene addition, the attached perylene crystals grew larger and started to show regular shapes. On the basis of the observed PANI-protected intermediates (Figure 5a–d), it appears that perylene growth was initiated at one or a few sites on an AuNP before completely engulfing it. Note that the nanocrystals in the TEM images were expected to have undergone slight/partial perylene dissolution, particularly for the small ones, because SDS (3.6 mM) was used to stabilize the PANI-coated nanocrystals during their purification.

In contrast to perylene growth, single-crystalline inorganic nanocrystals are much less known for tolerating defects, not to mention foreign particles. Hence, growth of the organic nanocrystals here is fundamentally different. In the previously proposed quasi-epitaxial growth of organic crystals on bulk inorganic substrates,[19] a key point was that aromatic organic molecules could distort or reorient at or near the interfaces. In doing so, the crystal could avoid major disruption of lattice structure, and thus the overall interfacial energy is reduced. We infer that the same principle (not the hetero-epitaxy) may also allow the perylene nanocrystals in our system to minimize the small defects along the Au/perylene interface and thus eventually grow around the huge

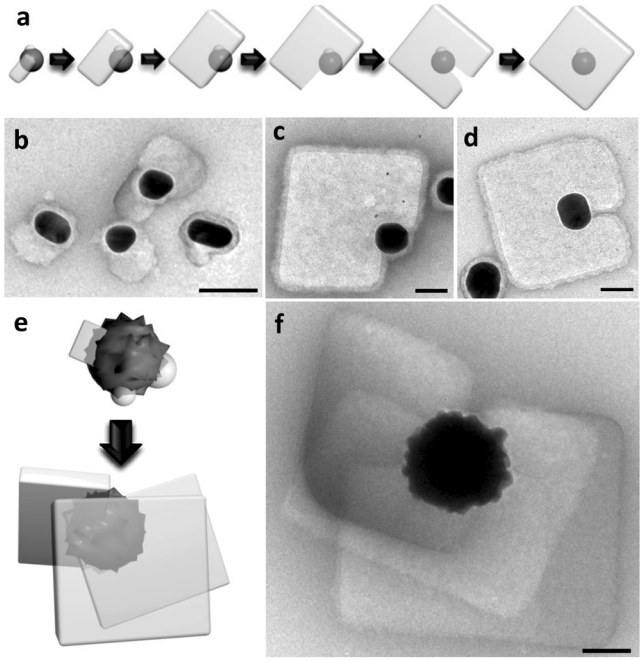

Figure 5. a) Schematics showing the proposed growth intermediates of AuNP@perylene before PANI encapsulation. b–d) TEM images of the observed PANI-trapped intermediates selected from control experiments with increasing perylene concentrations. e, f) Growth model and TEM image of (AuNF@perylene)@PANI with multiple twinned perylene crystals. Scale bars: 50 nm.

Au "defect". In comparison to the packing of metal atoms, the interactions among perylene molecules are weaker van der Waals forces. In addition, the perylene molecules are more flexible, less regular in shape, and require less specific coordination numbers in a lattice.[20] These differences can explain the unusual tolerance of the perylene nanocrystals for defects.

For the same reason, the growth of a dominant single-crystalline perylene phase is favored. In the event of multiple nucleation sites on one AuNP, the time difference in the random nucleation would mean that an earlier crystal will be slightly larger than the later ones. Given the small size of AuNPs, it is reasonable to expect the dominant phase to inhibit the growth of smaller neighboring ones. Thus, the small misaligned crystals could be engulfed by larger one as an additional impurity. However, if the AuNP seeds are large, two spatially separated nucleation sites would possibly have more opportunity to grow independently until they both become too large to be engulfed. On these seeds with large surface area, the probability to initiate multiple nucleation sites is also higher. This expectation was verified by experiments: When large AuNFs (100 nm) were used as seeds, more than 5% of them were found with multiple twined perylene nanocrystals (e.g., Figure 5f). This result is further evidence against Ostwald ripening: equilibration among the perylene nanocrystals in a solution should not be dependent on the size of the seeds to which they are attached.

In macroscopic crystals, incorporation of large impurity particles is actually not uncommon. For example, NaCl cubes

can often be found with embedded dirt or bubbles, though the size of such defects is usually much smaller than the surrounding single crystal. If a crystal grows large enough, it should always be able to grow around the defect and eventually engulf it. However, complete engulfing of crystallographically unmatched foreign material in nanoscale crystals is extremely rare.[21] Notably, smaller point defects embedded inside inorganic nanocrystals are very difficult to characterize, and so their occurrence is still an open question. From this perspective, incorporating large and high-density AuNPs in low-density organic crystals is an ideal model system for studying defect tolerance in single crystals.

In summary, we have reported an unconventional crystal growth that incorporated large polycrystalline AuNPs in single-crystalline perylene. Polyaniline encapsulation was used to protect and isolate the hybrid nanocrystals. On the basis of the trapped growth intermediates, we postulated that the ability of perylene to distort or reorient at Au/perylene interfaces allowed the perylene single crystals to grow around and accommodate large defects. This unconventional growth thus gives insights into defect tolerance in organic single crystals. Exploration in this direction could lead to dexterity in designing hybrid nanocrystals that are inaccessible by conventional crystal growth. Sophisticated hybrid nanocrystals are of great importance for exploring new physical properties and for recreating complex structural components for use in future nanodevices.

Received: May 1, 2011
Revised: June 28, 2011
Published online: September 5, 2011

Keywords: crystal growth · gold · nanoparticles · nanostructures · organic–inorganic hybrid composites

[1] a) Y. Xia, Y. J. Xiong, B. Lim, S. E. Skrabalak, *Angew. Chem.* **2009**, *121*, 62 – 108; *Angew. Chem. Int. Ed.* **2009**, *48*, 60 – 103; b) P. D. Cozzoli, T. Pellegrino, L. Manna, *Chem. Soc. Rev.* **2006**, *35*, 1195 – 1208; c) S. R. Forrest, *Nature* **2004**, *428*, 911 – 918; d) F. Wang, Y. Han, C. S. Lim, Y. H. Lu, J. Wang, J. Xu, H. Y. Chen, C. Zhang, M. H. Hong, X. G. Liu, *Nature* **2010**, *463*, 1061 – 1065.

[2] a) S. E. Habas, H. Lee, V. Radmilovic, G. A. Somorjai, P. Yang, *Nat. Mater.* **2007**, *6*, 692 – 697; b) S. X. Xing, Y. H. Feng, Y. Y. Tay, T. Chen, J. Xu, M. Pan, J. T. He, H. H. Hng, Q. Y. Yan, H. Y. Chen, *J. Am. Chem. Soc.* **2010**, *132*, 9537 – 9539; c) B. Lim, J. G. Wang, P. H. C. Camargo, M. J. Jiang, M. J. Kim, Y. N. Xia, *Nano Lett.* **2008**, *8*, 2535 – 2540; d) Y. J. Xiang, X. C. Wu, D. F. Liu, X. Y. Jiang, W. G. Chu, Z. Y. Li, Y. Ma, W. Y. Zhou, S. S. Xie, *Nano Lett.* **2006**, *6*, 2290 – 2294; e) L. Carbone, P. D. Cozzoli, *Nano Today* **2010**, *5*, 449 – 493; f) F. R. Fan, Y. Ding, D. Y. Liu, Z. Q. Tian, Z. L. Wang, *J. Am. Chem. Soc.* **2009**, *131*, 12036 – 12037.

[3] a) H. W. Gu, R. K. Zheng, X. X. Zhang, B. Xu, *J. Am. Chem. Soc.* **2004**, *126*, 5664 – 5665; b) H. W. Gu, Z. M. Yang, J. H. Gao, C. K. Chang, B. Xu, *J. Am. Chem. Soc.* **2005**, *127*, 34 – 35; c) H. Yu, M. Chen, P. M. Rice, S. X. Wang, R. L. White, S. H. Sun, *Nano Lett.* **2005**, *5*, 379 – 382; d) T. Pellegrino, A. Fiore, E. Carlino, C. Giannini, P. D. Cozzoli, G. Ciccarella, M. Respaud, L. Palmirotta, R. Cingolani, L. Manna, *J. Am. Chem. Soc.* **2006**, *128*, 6690 – 6698; e) J. Yang, H. I. Elim, Q. B. Zhang, J. Y. Lee, W. Ji, *J. Am. Chem. Soc.* **2006**, *128*, 11921 – 11926.

[4] a) F. R. Fan, D. Y. Liu, Y. F. Wu, S. Duan, Z. X. Xie, Z. Y. Jiang, Z. Q. Tian, *J. Am. Chem. Soc.* **2008**, *130*, 6949 – 6951; b) Z. Y. Zhang, M. G. Lagally, *Science* **1997**, *276*, 377 – 383; c) Z. M. Peng, H. Yang, *Nano Today* **2009**, *4*, 143 – 164; d) S. Torza, S. G. Mason, *J. Colloid Interface Sci.* **1970**, *33*, 67 – 83.

[5] See Supporting Information for details.

[6] a) M. X. Yang, G. Chen, Y. F. Zhao, G. Silber, Y. Wang, S. X. Xing, Y. Han, H. Y. Chen, *Phys. Chem. Chem. Phys.* **2010**, *12*, 11850 – 11860; b) S. X. Xing, L. H. Tan, M. X. Yang, M. Pan, Y. B. Lv, Q. H. Tang, Y. H. Yang, H. Y. Chen, *J. Mater. Chem.* **2009**, *19*, 3286 – 3291.

[7] H. Shinohara, Y. Yamakita, K. Ohno, *J. Mol. Struct.* **1998**, *442*, 221 – 234.

[8] a) G. Chen, Y. Wang, M. X. Yang, J. Xu, S. J. Goh, M. Pan, H. Y. Chen, *J. Am. Chem. Soc.* **2010**, *132*, 3644 – 3645; b) T. Chen, H. Wang, G. Chen, Y. Wang, Y. H. Feng, W. S. Teo, T. Wu, H. Y. Chen, *ACS Nano* **2010**, *4*, 3087 – 3094.

[9] a) F. J. M. Hoeben, P. Jonkheijm, E. W. Meijer, A. Schenning, *Chem. Rev.* **2005**, *105*, 1491 – 1546; b) Y. H. Feng, S. X. Xing, J. Xu, H. Wang, J. W. Lim, H. Y. Chen, *Dalton Trans.* **2010**, *39*, 349 – 351.

[10] L. H. Tan, S. X. Xing, T. Chen, G. Chen, X. Huang, H. Zhang, H. Y. Chen, *Acs Nano* **2009**, *3*, 3469 – 3474.

[11] a) H. R. Chung, E. Kwon, H. Kawa, H. Kasai, H. Nakanishi, *J. Cryst. Growth* **2006**, *294*, 459 – 463; b) J. Jang, J. H. Oh, *Adv. Mater.* **2003**, *15*, 977 – 980; c) X. J. Zhang, X. H. Zhang, W. S. Shi, X. M. Meng, C. Lee, S. Lee, *J. Phys. Chem. B* **2005**, *109*, 18777 – 18780.

[12] Y. Yin, A. P. Alivisatos, *Nature* **2005**, *437*, 664 – 670.

[13] a) H. Wang, J. Xu, J. H. Wang, T. Chen, Y. Wang, Y. W. Tan, H. B. Su, K. L. Chan, H. Y. Chen, *Angew. Chem.* **2010**, *122*, 8604 – 8608; *Angew. Chem. Int. Ed.* **2010**, *49*, 8426 – 8430; b) P. L. Soo, L. B. Luo, D. Maysinger, A. Eisenberg, *Langmuir* **2002**, *18*, 9996 – 10004; c) Y. Teng, M. E. Morrison, P. Munk, S. E. Webber, K. Prochazka, *Macromolecules* **1998**, *31*, 3578 – 3587.

[14] Y. N. Hong, J. W. Y. Lam, B. Z. Tang, *Chem. Commun.* **2009**, 4332 – 4353.

[15] T. Seko, K. Ogura, Y. Kawakami, H. Sugino, H. Toyotama, J. Tanaka, *Chem. Phys. Lett.* **1998**, *291*, 438 – 444.

[16] a) P. Li, Z. Wei, T. Wu, Q. Peng, Y. Li, *J. Am. Chem. Soc.* **2011**, *133*, 5660 – 5663; b) D. Z. Chen, R. M. Wang, I. Arachchige, G. Z. Mao, S. L. Brock, *J. Am. Chem. Soc.* **2004**, *126*, 16290 – 16291; c) R. Wang, I. U. Arachchige, S. L. Brock, G. Mao in *Nanoparticles: Synthesis Stabilization, Passivation, and Functionalization* (Eds.: R. Nagarajan, T. A. Hatton), ACS Symposium Series 996, American Chemical Society, New York, **2008**, pp. 358 – 368.

[17] a) F. Wang, C. Li, L.-D. Sun, H. Wu, T. Ming, J. Wang, J. C. Yu, C.-H. Yan, *J. Am. Chem. Soc.* **2011**, *133*, 1106 – 1111; b) A.-X. Yin, X.-Q. Min, Y.-W. Zhang, C.-H. Yan, *J. Am. Chem. Soc.* **2011**, *133*, 3816 – 3819.

[18] a) J. Ge, Q. Zhang, T. Zhang, Y. Yin, *Angew. Chem.* **2008**, *120*, 9056 – 9060; *Angew. Chem. Int. Ed.* **2008**, *47*, 8924 – 8928; b) T. Zhang, J. Ge, Y. Hu, Q. Zhang, S. Aloni, Y. Yin, *Angew. Chem.* **2008**, *120*, 5890 – 5895; *Angew. Chem. Int. Ed.* **2008**, *47*, 5806 – 5811.

[19] a) D. E. Hooks, T. Fritz, M. D. Ward, *Adv. Mater.* **2001**, *13*, 227 – 241; b) S. R. Forrest, *Chem. Rev.* **1997**, *97*, 1793 – 1896.

[20] F. Schreiber, *Phys. Status Solidi A* **2004**, *201*, 1037 – 1054.

[21] J. T. Zhang, Y. Tang, K. Lee, O. Y. Min, *Science* **2010**, *327*, 1634 – 1638.

